



Scholars Research Library

Archives of Applied Science Research, 2011, 3 (3):544-552

(<http://scholarsresearchlibrary.com/archive.html>)



Electrical Transport Properties in Carbon Nano Tube (CNT) as a channel of CNTFET

A. Bahari^{1,3}, Z. Naimi² and M. Amiri¹

¹Department of physics, University of Mazandaran, Babolsar, Iran

²Department of Science, Payam e noor university, Tehran, Iran

³School of Mathematical and Physical Sciences, University of Newcastle, Callaghan 2308, Australia

ABSTRACT

When a transistor is shrunk, all of its parts must be shrunk. When gate oxide is very slim, the current tunnelling to gate increases exponentially. The other problem in the current CMOS (Complementary Metal Oxide Semiconductor) transistor is the length of channel respect the Fermi wavelength. To make better and faster CPUs and logical device we need to use more transistors in an small area which have been faced with many challenges issues and problems due to tunnelling current and boron diffusion though the ultra thin silicon oxide film. Due to the importance of high current operations of electronic devices, Single Walled (SW) CNT has been considered as a one dimension (1D) structure and the strong covalent carbon-carbon bonding configuration. We have thus studied the electrical transport properties in a CNT as a channel of Carbon Nano Tube Field Effect Transistor (CNTFET) and simulated electron transport in a CNTFET by solving Boltzman equation to obtain distribution function in the SWCNT channel, including the development of high- κ gate dielectric integration, chemical functionalization for conformal dielectric deposition and pushing the performance limit of nanotube FETs by channel length scaling. The obtained simulations results show that in terms of ON state current density SWCNT can be choice as a wire for electron transportation compatibility with high- κ gate dielectrics. Our results show that system takes a stationary state after passing a time around 10^{13} s.

Keywords: Nano transistor, CNTFET, CNT and Electron Phonon Scattering

INTRODUCTION

According to Moore's law, the dimensions of individual devices in an integrated circuit have been decreased by a factor of approximately two every 18 months. Shrinking the size of devices down to 22 nm range has faced serious limits related to fabrication technology and device performances. The limits involve electron tunneling through short channels and ultra thin gate

dielectrics, the associated leakage currents, passive power dissipation, short channel effects and variations in device structure and doping [1-7]. These limits can be overcome to some extent and facilitate further scaling down of device dimensions by modifying the channel SWCNT [8-11].

Some researchers [9 -14] believed that SWNTs are advanced quasi-1D materials for future high performance electronics due to dependency of CNT bandgap on its chirality and diameter. If those properties can be controlled, CNTs would be a promising candidate for future nano-scale transistor devices. Moreover, because of the lack of boundaries in the perfect and hollow cylinder structure of CNTs, there is no boundary scattering. Because SWCNT is a quasi-1D material only forward scattering and back scattering are allowed, in that elastic scattering mean free paths in CNTs are long, typically on the order of micrometers, i.e., quasi-ballistic transport can be happened in SWCNTs at relatively long lengths and low fields [12].

There are typical bondings between a carbon atom in a graphene and its neighboring atoms which each carbon atom has three neighboring atoms to which it is connected. The rule explored in the present work is based on transport of carriers through the SWCNT.

Moreover, CNTFETs can have nearly maximum on/off current ratios. Its intrinsic switching time is about 100 fs. Monte Carlo simulations have been performed on CNTFET to get a better on/off switch time which can cause the improvements in stability and sensitivity of process variations and performance. The present work reports a shorter on-off switch time (10^{-13} s) in comparison to 0.1-1 ns of the current devices.

Theory

In numerous papers [10 – 17], CNT is considered a honeycomb lattice of a graphene sheet rolled into a cylinder. Graphene is also the name commonly associated with a single layer of graphite in two dimensions. The graphene sheet lattice structure is not a Bravais lattice by itself, but can be regarded as an underlying square Bravais lattice with a two – atom basis.

As mentioned previously, graphene is a two dimensional sheet consisting of connected carbon atoms in hexagons like the benzene molecule. The basis of a graphene sheet as shown in figure1, consists of two atoms named ‘a’ and ‘b’. When considering only nearest neighbor interaction between e.g. the ‘a’ atom and the nearest neighbors, which are three ‘b’ atoms, the angle between each ‘b’ atom is equally spaced with 120° . When folding the graphene sheet into a SWCNT it is possible to use the concepts and calculations from graphene sheets[13].

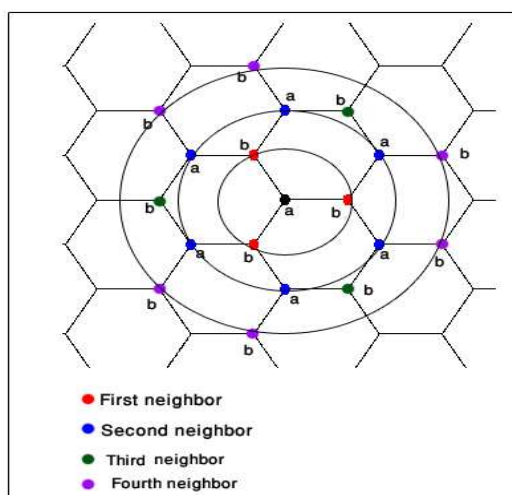


Figure1. Neighbor atoms of a graphitic plane up to 4th nearest neighbors for an ‘a’ atom. Circles connecting the same neighbor atoms are for guides to the eye.

Indeed, the calculations are performed on graphene sheets, which is a good approximation if the radius of the CNT can be much greater than the distance between two neighboring nuclei of the carbon atoms in the CNT. As we know from the literature like [14, 15], the diameter of most CNTs is between 0.7 nm and 2 nm, whereas the distance between the nuclei of the atoms is 1.42 Å.

Here we concentrate on the 'velocity Verlet' algorithm, which may be written [16-17]

$$p_i \left(t + \frac{1}{2} \delta t \right) = p_i(t) + \frac{1}{2} \delta t f_i(t) \quad (1a)$$

$$r_i(t + \delta t) = r_i(t) + \frac{\delta t p_i \left(t + \frac{1}{2} \delta t \right)}{m_i} \quad (1b)$$

$$p_i(t + \delta t) = p_i \left(t + \frac{1}{2} \delta t \right) + \frac{1}{2} \delta t f_i(t + \delta t) \quad (1c)$$

After step (1b), a force evaluation is carried out, to give $f_i(t + \delta t)$ for step (1c). This scheme advances the coordinates and moments over a time step δt .

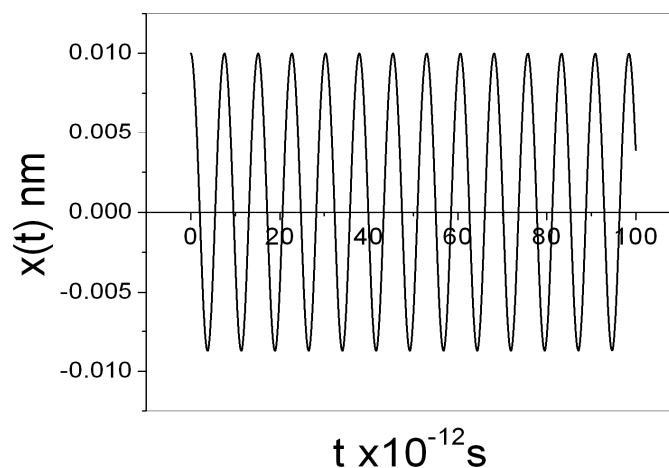


Figure 2. Vibration of arbitrary atom. We consider the effect of just first nearest neighbor's atoms on the atom.

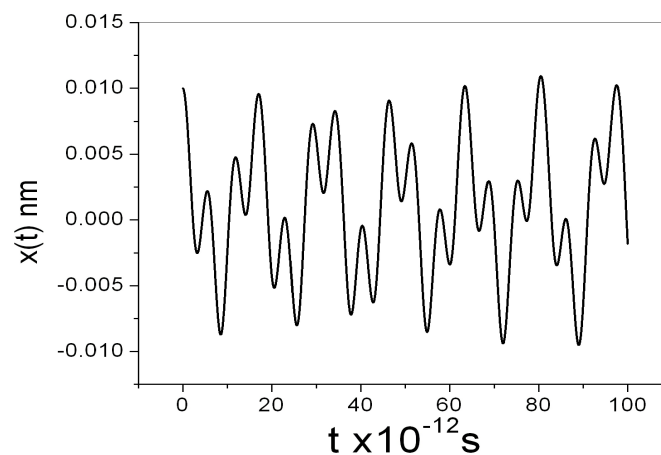


Figure 3. Displacement of arbitrary atom. We consider the effect of just first nearest neighbor's atoms on the atom.

Figures 2 and 3 show the displacement of arbitrary atom which plotted based on velocity Verlet algorithm. It represents harmonic vibrations with the same amplitude, direction and phase, where only arbitrary atom is allowed to move or vibrates. Now we assume an electric field is applied to a CNT transistor, and then a mobile charge is induced in the tube from the source and drain. These charges are from the density of positive velocity states filled by the source N_S and that of negative velocity states filled by the drain N_D [6], and these densities are determined by the Fermi-Dirac probability distributions and the equilibrium electron density is where the density of states at the channel $D(E)$. In fact, SWCNT is affected by external terminal voltages which are implicitly related to the device terminal voltages, charges at terminal.

According to the CNT ballistic transport theory, we can conclude that the drain current caused by the transport of the nonequilibrium charge across the channel of CNTFET. Up to now, calculations for finding the phonon dispersion relations of CNTs have been performed with using tight-binding methods [18], density functional theory [19] and symmetry-adapted models [20]. It can also be understood by using zone folding of the phonon dispersion branches of graphene. However in the present work, we calculate the phonon dispersion of a graphene sheet by using modified force constant model [21] and considering the effect of 4 nearest neighbour's carbon atoms. Since there are two carbon atoms in the unit cell of graphene, one must consider 6 coordinates. The secular equation to be solved is thus a dynamical matrix of rank 6, such that 6 phonon branches are achieved. Figure 4 shows phonon energy relation of graphene along high symmetry lines. It shows phonon dispersion relation of graphene along high symmetry lines.

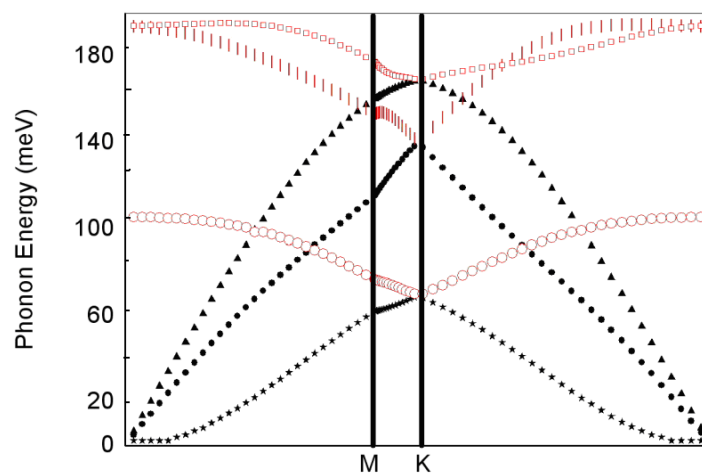


Figure 4: Phonon dispersion of graphene along high symmetry points.

We assume CNT is a perfect structure net without any crystal defects. Therefore the transport should be considered a ballistic transport in that it yields to important diffusion transport [22]. Although ballistic transport has been taken place in the metallic type of CNT, it can also be occurred in the semi conducting CNT. We therefore calculate the scattering rate of electron-phonon scattering process by using Fermi golden rule [23] and scattering rate, given by

$$W_{\vec{k},\vec{k}'}^{op} = \frac{D_{op}^2 \cdot DOS(\vec{k}')}{\rho \cdot d \cdot \omega_p} \left(N_p + \frac{1}{2} \pm \frac{1}{2} \right) \quad (2)$$

$$W_{\vec{k},\vec{k}'}^{ac} = q^2 \frac{D_{ac}^2 \cdot DOS(\vec{k}')}{\rho \cdot d \cdot \omega_p} \left(N_p + \frac{1}{2} \pm \frac{1}{2} \right) \quad (3)$$

Where N_p is Bose-Einstein occupation number, ρ is mass density of graphene sheet, D is deformation potential, d is CNT diameter and q is phonon wave vector [23]. To determine electron-phonon scattering rates, electron band structure and phonon dispersion are divided into 2000 grid points covering first BZ. The requirements of energy and momentum conservations lead to following selection rules for final electron state.

$$E_f = E_i \pm E_{ph} \quad (4)$$

Where \vec{k} refers to electron and \vec{q} refers to phonon wave vector. Distribution function of electron or hole can be varied under applied electric or magnetic fields and scattering phenomena. Moreover, the carrier transport in single-walled semi conducting carbon nanotubes is then found by solving the Boltzmann equation [22, 23];

$$\frac{\partial g_n(\vec{r}, \vec{k}, t)}{\partial t} + \vec{v} \cdot \vec{\nabla}_r g_n(\vec{r}, \vec{k}, t) + \vec{F} \cdot \vec{\nabla}_k g_n(\vec{r}, \vec{k}, t) = \sum_{\vec{k}'} [W_{\vec{k},\vec{k}'} g_n(\vec{r}, \vec{k}, t) (1 - g_n(\vec{r}, \vec{k}', t)) - W_{\vec{k}',\vec{k}} g_n(\vec{r}, \vec{k}', t) (1 - g_n(\vec{r}, \vec{k}, t))] \quad (5)$$

It is now possible to simplify Eq.5 by using relaxation time approximation [24].

$$\frac{\partial g_n(\vec{r}, \vec{k}, t)}{\partial t} + \vec{v} \cdot \vec{\nabla}_r g_n(\vec{r}, \vec{k}, t) + \vec{F} \cdot \vec{\nabla}_k g_n(\vec{r}, \vec{k}, t) = - \frac{g_n(\vec{r}, \vec{k}, t) - g_n^0(\vec{r}, \vec{k}, t)}{\tau} \quad (6)$$

Where g_n^0 is initial distribution function of n^{th} branch of energy dispersion of CNT. It is independent on scattering phenomena and applied field. We now assume a Fermi-Dirac distribution function for unaffected electron. For longer CNT channel (respect to Debye wavelength), the distribution function will be independent on \vec{r} (displacement vector) which leads to

$$g_{n,el}^0(k, t) = f_{n,el}^0(k) = \frac{1}{e^{\frac{E_n(\vec{k}) - \mu}{k_B T}} + 1}$$

$$g_{n,ho}^0(k, t) = 1 - f_{n,el}^0(k) \quad (7)$$

Where $E_n(\vec{k})$ is electron energy. The wave function of electron is assumed as a Bloch function and the velocity of electrons can be thus obtained from semi classical motion relation as below [25]

$$V_n(\vec{k}(t)) = \frac{1}{\hbar} \vec{\nabla}_k E_n(\vec{k}, t) \quad (8)$$

In this simulation we take a common drift time for all electrons, $t_d = 10^{-15}$ s and assumed that Fermi level is a constant value both at the electric field and scattering mechanism. This assumption makes a limitation on charge density in presence of electric field. As stated above, although the distributions function is deviated from its primary Fermi-Dirac shape we focused a point on the Fermi level in where there are allowed transitions between energy levels, at the $t = 0$

– 10^{-13} s. This fact indicates unstable condition so that we need to obtain the scattering phenomena randomly based on electrons-holes positions. Furthermore, the average velocity is given as below;

$$\bar{V} = \sum_i V_i g_n(k_i, t_i)$$

Where $t_i = it_d$ and the average of current is calculated via

$$n(t) = 2 \times 2 \times \frac{|T|}{2\pi} \sum_v \int_{-\frac{\pi}{T}}^{\frac{\pi}{T}} g_v(k, t) dk$$

and

$$\bar{n} = \frac{1}{t} \int_0^t n(t') dt'$$

$$I_{DS} = |\bar{n} e \bar{v}| \tag{9}$$

In this situation, the system trends to a stationary state with below electric current

$$I = 2 \times 2 \times \frac{|T|}{2\pi} \int_{-\frac{\pi}{T}}^{\frac{\pi}{T}} g_v(k) V_v(k) dk \tag{10}$$

Where 2×2 are due to spin and the double degeneracy of the first conduction band in zigzag type of CNTs.

DISCUSSIONS

The calculated results are revealed in figures 2 through 8. Figure 5 shows time dependent of distribution function on wave vector. It indicates that the distribution function is initially obeyed Fermi-Dirac function, but after passing 10^{-13} s, leads to the self limiting and/ or Boltzman function behaviour, meaning the system is an unstable case which can be confirmed by looking at figure 6.

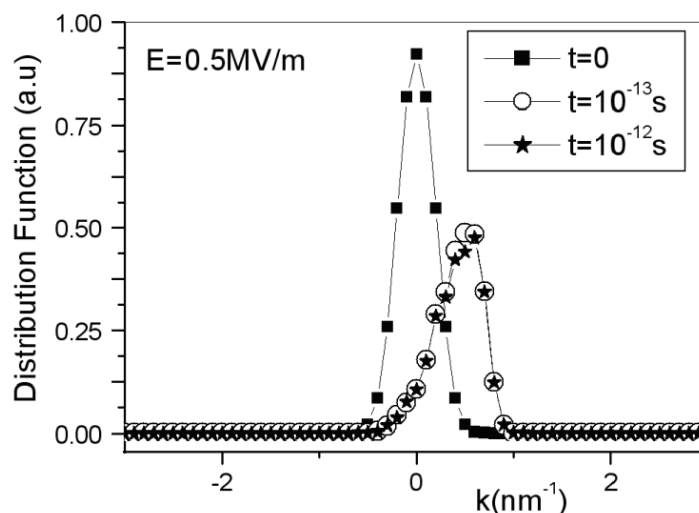


Figure 5: Distribution function takes a uniform shape.

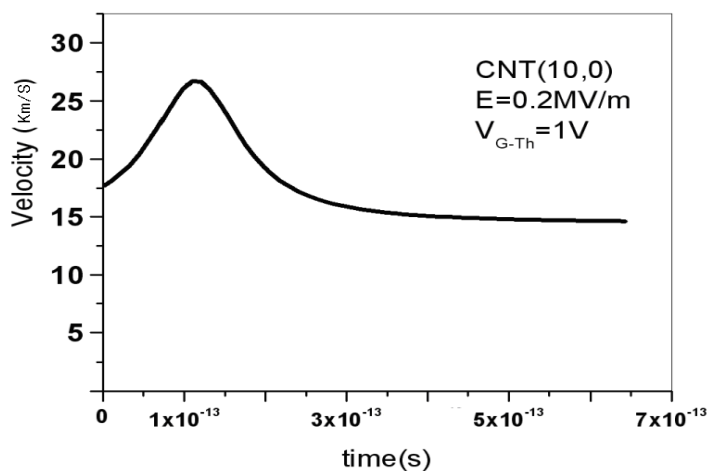


Figure 6: Time dependent of carrier velocity.

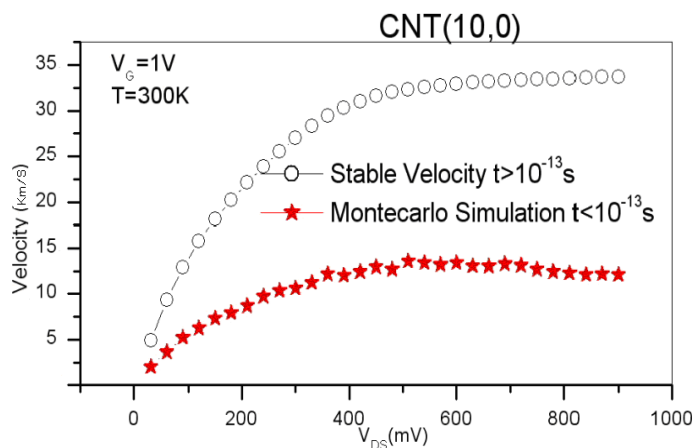


Figure 7: Comparison of the stable and instable velocities.

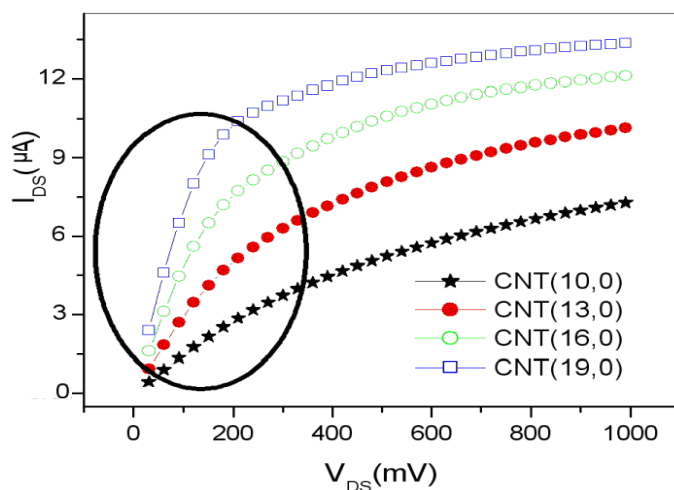


Figure 8: Comparison of the current for different diameters of CNTs.

Figure 6 shows time dependent velocity of electron in a CNT(10,0), as an example, so that the electron velocity trends a Sigmoid behaviour after 2×10^{-13} s. We compared carrier velocity versus drain – source voltage in figure 7 to show different behaviour of carrier transport through

the SWCNT channel. The curves indicate the significant of carrier transport in on/off switching time for an ensemble consisting of 1000 electrons. The other important result of present work is shown in figure 8. It obviously indicates that by increasing CNT diameter, the carrier current through increases as labelled by circle in figure and demonstrates a rather violent slope at $0 - 10^{13}$ s range, in when the best voltage in this case is one volt for a gate-voltage.

Furthermore, there are so strong covalent carbon-carbon bonding in the sp^2 configurations which cause CNTs be chemically inert and able to transport large amounts of electric current. The results show that semiconducting SWCNT are preferred over metallic single-walled and metallic multi-walled tubes since they are able to be fully switched off, at least for low source/drain biases. The strong covalent C-C bonding and lack of surface dangling bonds are the fundamental reasons underlying the advanced properties of carbon nanotubes and high potential for future electronics.

CONCLUSIONS

We present our recent progress in developing gate dielectric integration and channel length scaling for SWNT FETs. Some issues such as tunnelling and leakage current and boron diffusion through the ultra thin gate dielectric are threatening the use of silicon dioxide to be used for the future of CMOS devices, because it can degrade the performance of the conventional devices. In fact, they can no longer operate properly. Revolutionary concepts; therefore, need to be developed for further miniaturization of digital components down to the molecular scales. The most desirable future work involved in CNTFETs will be the transistor with higher reliability after studying the effects external to the inner CNT transistor like the Schottky barrier between the CNT and metal contacts, multiple CNTs at a single gate.

In conclusion future race of CNTFETs has a magic speed and shorter size. The present work, as shown in above figures, the on-off switch can be good switching time for a CNT, at nearly 10^{-12} s, meaning the CNTFET can be switched faster than that current MOSFET.

REFERENCES

- [1] A. Rahman, J. Guo, S. Datta, Fellow, IEEE and M. S. Lundsturm, *Tran. Electron Dev.*, 50 (2003) 1853-1864.
- [2] R. Saito, G. Dresselhaus and M. S. Dresselhaus, *Physical Properties of Carbon Nanotubes*, ISBN: 1-86094-093-5 (1998).
- [3] A . Bahari, *Acta Phys. Polonica A*, 115 (2009) 622-25.
- [4] A . Bahari and M. Amiri, *Acta Phys. Polonica A*, 115 (2009) 625 -628.
- [5] C. Zhihong, F. Damon, X. Sheng, G. Roy, A. Phaedon and J. Appenzeller, *IEEE Electron De. Lett.*, 29 (2008) 183 -195.
- [6] C. Jian, S. Kuo, H. Jeng-Rong and J. Cheng, *Microelectr. Engin.*, 87(2010)1973 -83.
- [7] P. Eric, D. Sumit, E. David and L. Albert, *Nano Sci. Technol. Series*, 12 (2009) 405 - 412.
- [8] A. Bahari, P. Morgen and Z. S. Li, *Surf. Sc.*, 602 (2008) 2315-2324.
- [9] A. Bahari, U. Robenhagen, P. Morgen and Z. S. Li, *Phys. Rev. B.*, 72 (2005) 205323-331.
- [10] X. Qi, M. Wei, Y. Lin, Q. Jia, D. Zhi, J. Dho, M. G. Blamire and J. L. MacManus-Driscoll, *Appl. Phys. Lett.*, 86 (2005) 071913-916.
- [11] S. Heinze, J. Tersoff, R. Martel, V. Derycke, J. Appenzeller and P. Avouris, *Phys. Rev. Lett.*, 89 (2002) 106801 -12.

- [12] P. Avouris and J. Chen, International Technology Roadmap for Semiconductors, *Materials Today*, 9 (2009) 46 - 50.
- [13] L. Yu-Ming, T. James, C. Freitag and A. Phaedon, *Nanotechnology*, 18 (2007) 295202 - 215.
- [14] R. A. Jishi, D. Inomata, K. Nakao, M. S. Dresselhaus, and G. Dresselhaus, *J. Phys. Soc. Jap.*, 63 (1994) 2252-2260.
- [15] V. N. Popov and P. Lambin, *Phys. Rev. B.*, 73 (2006) 085407-424.
- [16] J. Yu, R. K. Kalia, and P. Vashishta, *J. Chem. Phys.*, 103 (1995) 6697-6705.
- [17] M. Menon, E. Richter, and K. R. Subbaswamy, *J. Chem. Phys.*, 104 (1995) 5875-5882.
- [18] P. C. Eklunda, J. M. Holdena and R. A. Jishi, *Carbon*, 33 (1995) 959-972.
- [19] O. Dubay and G. Kresse, *Phys. Rev. B.*, 67 (2003) 035401-410.
- [20] V. N. Popov, V. E. V. Doren and M. Balkanski, *Phys. Rev. B.*, 59 (1999) 8355-8358.
- [21] A. Grouneis, R. Saito, T. Kimura, L. C. Cancado, M. A. Pimienta, A. Jorio, A. G. Souza Filho, G. Dresselhaus and M. S. Dresselhaus, *Phys. Rev. B.*, 65 (2002) 155405-415.
- [22] Y. F. Chen and M. S. Fuhrer, *Phys. Rev. Lett.*, 95 (2005) 236803-882.
- [23] G. Pennington and N. Goldsman, *Phys. Rev. B.*, 68 (2003) 45426-437.
- [24] D. V. Pozdnyakov, V. O. Galenchik, F. F. Komarov and V. M. Borzdov, *Physica E*, 33 (2006) 336-342.
- [24] N. W. Ashcroft and N. D. Mermin, *Solid State Phys*, ISBN: 0-03-083993-9 (1976).
- [25] Zh. Yao, Ch. L. Kane and C. Dekker, *Phys. Rev. Lett.*, 84 (2000) 2941-953.